

# Controlling Carbodiimide-Driven Reaction Networks Through the Reversible Formation of Pyridine Adducts

William S. Salvia, Georgia Mantel, Nirob K. Saha, Chamoni W. H. Rajawasam, Dominik Konkolewicz\*, C. Scott Hartley\*

Department of Chemistry & Biochemistry, Miami University, Oxford, OH 45056, United States  
scott.hartley@miamioh.edu

## Abstract

Carbodiimide-driven anhydride formation from carboxylic acids is useful in a variety of non-equilibrium systems. While multiple strategies to control deactivation rates (anhydride hydrolysis) have been reported, control over activation rates (anhydride formation) is currently limited. We show that pyridines reversibly form adducts with 1-ethyl-3-(3-dimethylaminopropyl)carbodiimide methiodide in water. These adducts are unreactive with carboxylic acids and thus reduce the anhydride formation rate while prolonging carbodiimide lifetime. The best results are obtained with 4-methoxypyridine. This strategy can be used to control the formation of transient polymer network hydrogels, in one example increasing the time to reach peak modulus by 86% and the lifetime by 43%.

Responsive materials and molecular machines can be realized through non-equilibrium reaction networks operating through transient covalent bonds formed by “fueling” reactions.<sup>1,2</sup> The design of responsive systems is facilitated by the development of fuel reactions that can be broadly applied in different systems. While several options have now been identified,<sup>1,3–5</sup> the hydration of carbodiimides is among the most useful.<sup>6,7</sup> These systems usually function through the formation of anhydrides, which hydrolyze in aqueous media. Carbodiimide chemistry has been applied to a diverse array of non-equilibrium systems, including transient hydrogels,<sup>8–12</sup> droplets,<sup>13</sup> molecular machines,<sup>2,14–19</sup> supramolecular systems,<sup>7,20</sup> polymer networks,<sup>8,21,22</sup> and DNA hybridization.<sup>23</sup> In almost all cases, the carbodiimide used in these systems is 1-ethyl-3-(3-dimethylaminopropyl)carbodiimide hydrochloride (EDC).<sup>8,10,13,17,20,24,25</sup> However, as shown in Scheme 1a, EDC is arguably not a true carbodiimide—it undergoes ring-chain tautomerization under typical conditions for nonequilibrium systems and is perhaps best described as a guanidinium cation.<sup>26</sup> Another commercially available carbodiimide, 1-ethyl-3-(3-(dimethylamino)propyl)carbodiimide methiodide (mEDC),<sup>27</sup> is analogous to EDC but unable to cyclize. Consequently, mEDC is much more susceptible towards hydrolysis at most pHs,<sup>26</sup> and more reactive with carboxylic acids and strong amines.<sup>28</sup> It is, however, rarely used in nonequilibrium systems chemistry.<sup>15</sup>

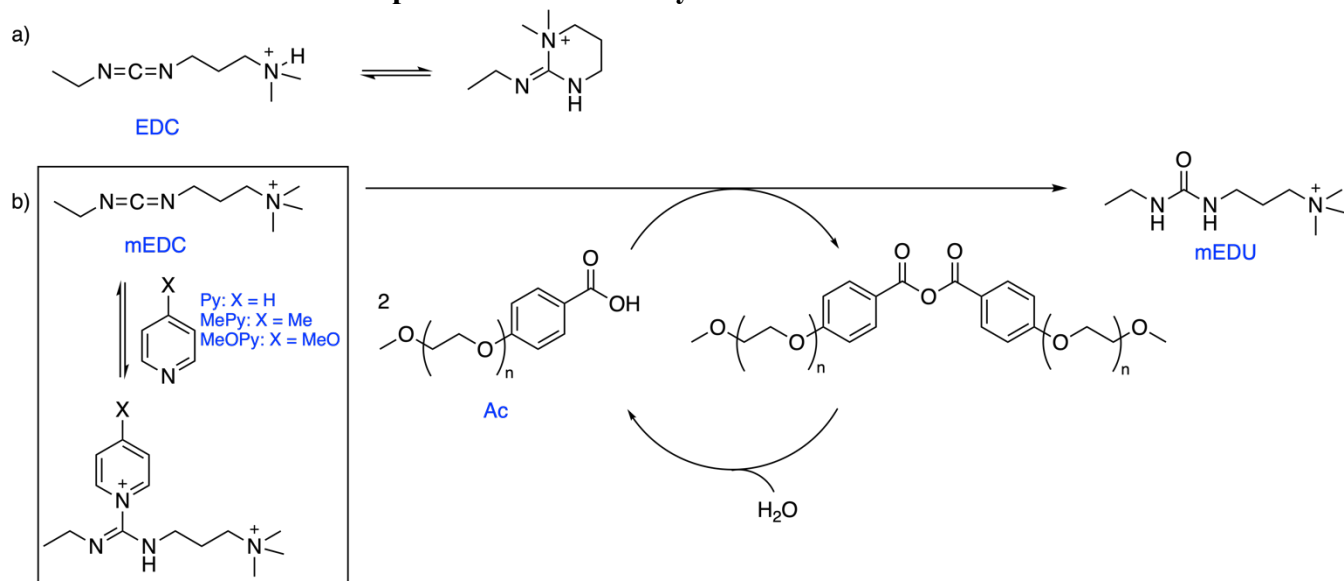
Kinetic control underlies all nonequilibrium reaction networks, and thus controlling the rates of the component reactions is of critical importance. Substrate effects,<sup>29</sup> product phase separation,<sup>13</sup> and careful design of transient assemblies<sup>11</sup> can be used to control anhydride hydrolysis (deactivation) rates in carbodiimide-driven systems. Control over anhydride formation (activation) rates is less common, and is so far restricted to the variation of the carbodiimide used, with limited success to date.<sup>6,17,30</sup> Using entirely different carbodiimide structures limits system tunability, especially because few water-soluble carbodiimides are commercially available. This limitation contrasts with a greater degree of control observed in biological systems. ATP, the prototypical biological chemical fuel, is regulated via its synthesis and

storage,<sup>31</sup> and not generally structural variation. One method of reversibly storing ATP in an inactive state is by the temporary covalent inactivation of kinases.<sup>32,33</sup> While not exactly the same strategy, a reversible covalent inhibitor for a carbodiimide would be a general approach to controlling its availability in nonequilibrium reaction networks.

Here, we show that mEDC reversibly forms inert adducts with pyridines, affording straightforward control over carbodiimide-driven reaction networks. By reducing the mEDC's effective concentration, the rate of anhydride formation is reduced. At the same time, the adducts act as inactive reservoirs of carbodiimide to extend overall system lifetimes. We demonstrate these concepts in a prototypical transient polymer network hydrogel.

Pyridine (Py) is often added to carbodiimide-driven reaction networks, both as a buffer and to inhibit the formation of undesirable *N*-acylurea byproducts.<sup>34</sup> When monitoring reactions of mEDC in the presence of Py, we noticed unexpected NMR signals that decayed over the course of the experiment. As shown in Figures 1 and S7-8, in the absence of carboxylic acid this new species forms immediately and then is lost at the same rate as the mEDC itself. We assigned the new species as the pyridine–mEDC adduct, formed as in Scheme 1b, based on NMR assignments (Figures S7-8) and its detection in the reaction mixture by MS (Figure S6). Nucleophilic attack on carbodiimides by amines, including triethylamine,<sup>35</sup> arylamines,<sup>36</sup> piperidine,<sup>37</sup> and imidazole,<sup>37</sup> is well-precedented (not to mention EDC's intramolecular cyclization, Scheme 1a<sup>26</sup>). However, in these cases the adducts are either unobserved reactive intermediates<sup>35</sup> or thermodynamically stable products.<sup>36,37</sup> Importantly, EDC itself does not form adducts with pyridine (Figure S12), presumably because of competition from its cyclization. The mEDC adduct concentration increased roughly threefold when the Py concentration was increased from 100 to 300 mM (Figure S40).

**Scheme 1. (a) Ring-chain tautomerization of EDC and (b) adduct formation from mEDC coupled to transient anhydride formation.**



Pyridine gives a relatively low concentration of adduct; hence, we also tested more nucleophilic 4-methylpyridine (MePy) and 4-methoxypyridine (MeOPy) derivatives.<sup>38</sup> As shown

in Figures 1 and S39, adducts are formed when Py, MePy, or MeOPy are treated with an aqueous solution of mEDC, with higher adduct concentrations as pyridine nucleophilicity increases. Figure 1 compares the net mEDC available in the system (black lines); with increasing adduct concentration, the overall consumption of mEDC is slower. After ~20 min, about 40% of the MeOPy's total mEDC was consumed, compared to about 60% for Py.

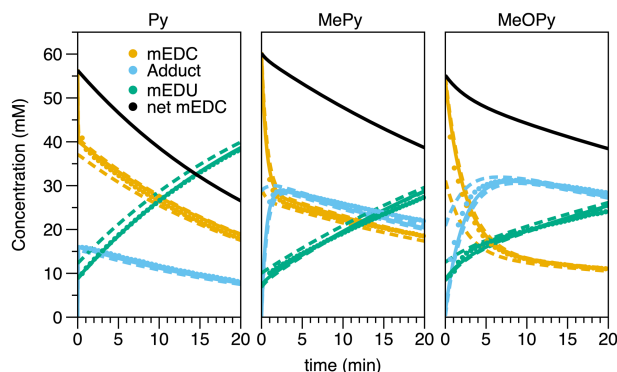


**Figure 1.** Change in concentrations over time for 300 mM Py, MePy, and MeOPy treated with 75 mM mEDC in D<sub>2</sub>O at pH 5.5 and room temperature. The net mEDC (black) is the sum of the mEDC (orange) and adduct (blue) fits. Datapoints, fits, and 95% confidence intervals (dashed lines) are depicted for each species.

The concentration vs time plots for all three systems can be fit to a simple mechanism:<sup>29</sup>



As expected,  $k_5$  is indistinguishable with all three pyridines (Py: 3.2 s<sup>-1</sup>, MePy: 2.7 s<sup>-1</sup>, MeOPy: 2.9 s<sup>-1</sup>). For Py, adduct formation ( $k_4$ ) and decomposition ( $k_{-4}$ ) are fast and thus only their ratio,  $K$  ( $k_4/k_{-4}$ ), can be determined from our data. For MePy and MeOPy, these reactions are slower and  $k_4$  and  $k_{-4}$  can be separately extracted (Table S1). The rate of formation ( $k_4$ ) decreases in the order Py > MePy (180 M<sup>-1</sup> s<sup>-1</sup>) > MeOPy (55 M<sup>-1</sup> s<sup>-1</sup>). This can be justified by the more nucleophilic pyridines being deactivated by protonation at pH 5.5 (see Supporting Information). The rate of decomposition of the adduct ( $k_{-4}$ ) follows the same trend, with Py > MePy (47 s<sup>-1</sup>) > MeOPy (7.2 s<sup>-1</sup>). That is, electron-donating groups stabilize the adduct. Despite the similar trends in  $k_4$  and  $k_{-4}$ , the ratio  $K$  increases in the order Py (1.4 M<sup>-1</sup>) < MePy (3.8 M<sup>-1</sup>) < MeOPy (7.6 M<sup>-1</sup>), and so more adduct accumulates for increasingly electron-donating substituents (Figure S78).<sup>39</sup>

To establish that adduct formation is orthogonal to carbodiimide-driven anhydride formation, and thus can both slow anhydride activation and establish an mEDC reservoir, we tested the complete reaction network in Scheme 1 using benzoic acid Ac as a simple model (avg.  $n = 11-12$ ).<sup>7</sup> Its anhydride was independently synthesized for reference (Figure S4).

Despite its slower on/off kinetics, MeOPy provides the highest concentration of adduct in the presence of Ac. In a typical experiment, MeOPy and mEDC were combined in D<sub>2</sub>O and allowed to stand for 5 min to give time for the adduct to fully form. Without this premixing, the adduct concentration was much lower (Figure S74). This solution was then added to a solution of

Ac. As a control, the reaction was carried out using EDC in place of mEDC, since EDC does not form the adduct. A control without MeOPy is not possible, since it affects other parts of the reaction network (e.g., catalyzing anhydride hydrolysis, see Eq 3-7) and acts as the buffer.

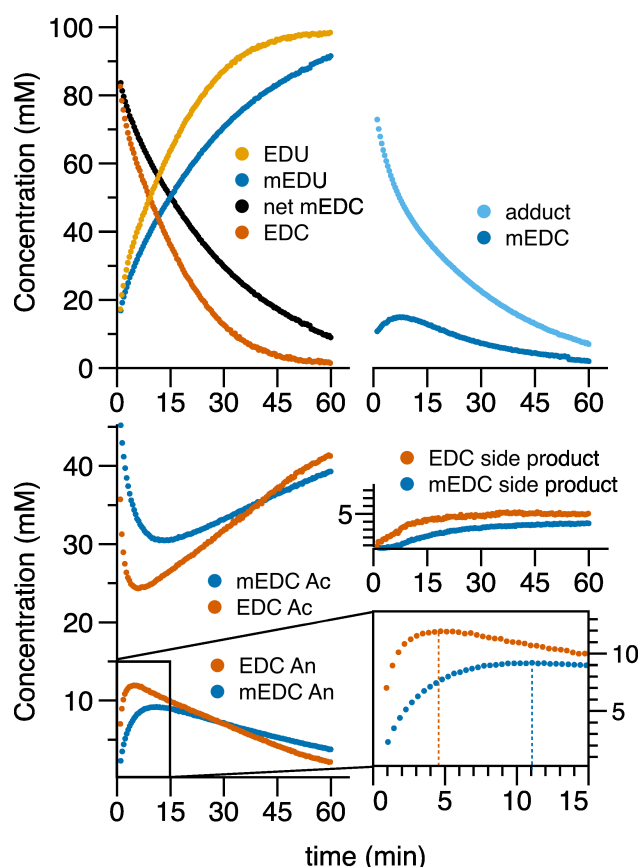
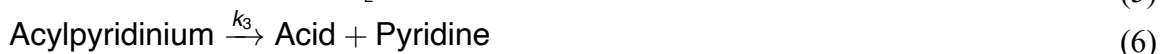
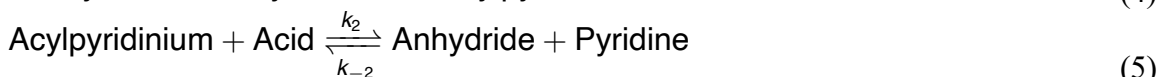
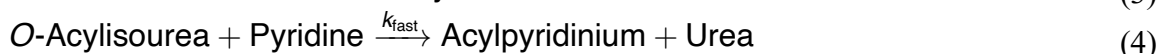


**Figure 2.** Changes in concentrations over time for 100 mM mEDC vs EDC in 300 mM MeOPy with 75 mM DMA in D<sub>2</sub>O at pD 5.5 and room temperature. The timescale is truncated for the mEDC experiment (see Figure S75).

Notably, in the mEDC sample, when compared to the EDC sample, the rate of formation of the anhydride was slower and its lifetime was longer, as shown in Figure 2. With mEDC, the anhydride reached its peak concentration at 11 min, compared to 4.7 min for EDC, a 134% increase, which resulted in a 17% decrease in peak anhydride concentration as anhydride formation competed less effectively with hydrolysis. Further, the net mEDC is lost more slowly than the EDC, despite mEDC's inherent increased reactivity. The concentration of free mEDC was consistently low (<15 mM) but it was continuously released from the adduct. The anhydride persisted longer for mEDC relative to the EDC because the adduct acts as a carbodiimide reservoir. The lifetimes, defined as the time taken for the Ac to return to 80% of its original value, were 63 min and 53 min for mEDC and EDC, an approximately 20% increase. A small amount of an unknown side product was found in both the EDC (4.6 mM) and mEDC (3.4 mM) systems. It is longer-lived than the anhydride but transient, decomposing back to Ac after one day (Figure S76).

The mechanism in Eq 3–8, assuming a steady-state in the acylpyridinium ( $\alpha = k_2/k_3$ ) and that  $k_{\text{fast}} \gg k_1$ , successfully fits the data for all three pyridines (see Eq S12–S26). In addition to adduct formation, the pyridines directly affect anhydride hydrolysis.



Unfortunately, the parameters  $\alpha$  and  $k_{-2}$  are correlated in these fits and cannot be determined from the experimental data alone. That is, the model cannot determine whether anhydride both forms and decomposes fast or slow. However, Ferscht and Jencks have reported values  $k_{-2}$  for the hydrolysis of acetic anhydride by Py, MePy, and MeOPy, which we can use to determine the general substituent effect on  $\alpha$  (Table S3).<sup>40</sup> This previous work suggests that the parameter  $k_{-2}$  (Eq 5) increases from Py to MePy to MeOPy, meaning that more electron-rich pyridines attack more quickly. While acetic anhydride undergoes hydrolysis much faster than benzoic acid Ac,<sup>41</sup> the trend likely holds. In the present work, this suggests that  $\alpha$  is independent of the type of pyridine used (Table S3). As more nucleophilic pyridines are used, the increased value of  $k_{-2}$  leads to a faster breakdown and decreased concentration of the anhydride (Figure S77).

To establish that mEDC–pyridine adducts can affect the behavior of a functional system, the carbodiimide-driven crosslinking of poly(DMAM<sub>70</sub>-AA<sub>30</sub>), shown in Figure 3a, was used as a model. On treatment with carbodiimide, a solution of poly(DMAM<sub>70</sub>-AA<sub>30</sub>) forms a polymer network hydrogel through the generation of anhydride crosslinks from the pendant carboxylic acid groups.<sup>21</sup> The gel eventually returns to a liquid state as the anhydride linkages hydrolyze. 500 mM of mEDC along with 100 mM MeOPy were added to an aqueous solution of poly(DMAM<sub>70</sub>-AA<sub>30</sub>). This provides an initial 400 mM of free carbodiimide to initiate gelation (determined from preliminary experiments) along with an additional 100 mM to serve as a reservoir through the formation of adduct. As before, the MeOPy and mEDC were premixed for 5 min before addition to the hydrogel to allow the adduct concentration to peak.

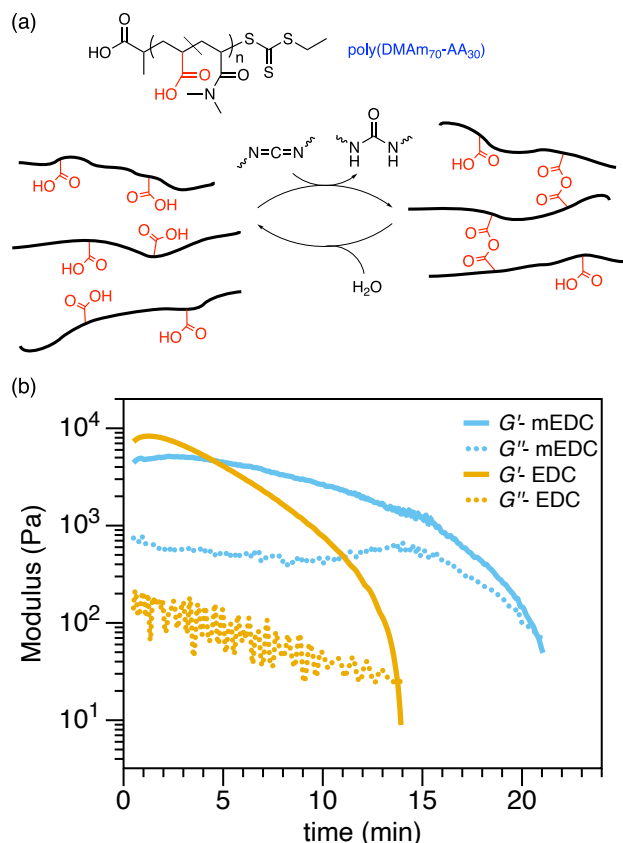


**Figure 3.** a) Hydrogel structure both under equilibrium and non-equilibrium conditions. b) Storage ( $G'$ , solid) and Loss ( $G''$ , dashed) modulus over time for mEDC (blue) and EDC (orange).

Figure 3 shows the rheological time sweep data for gelation and degelation of poly(DMAM<sub>70</sub>-AA<sub>30</sub>). As before, EDC was used as a control as it does not form an adduct with MeOPy. On addition of carbodiimide, both systems underwent rapid gelation, as indicated by storage moduli ( $G'$ ) greater than loss moduli ( $G''$ ). With mEDC, the peak  $G'$ , which corresponds to the peak anhydride crosslink density, occurred at 130 s, compared to 70 s with for EDC, an 86% increase. The peak  $G'$  was also noticeably lower for mEDC compared to EDC. Similarly, the hydrogel had a substantially longer 20 min lifetime with mEDC, compared to 14 min for EDC, a 43% increase. These results are consistent with the effects of adduct formation in the mEDC system. The delayed and lower peak  $G'$  implies a slower activation rate compared to EDC because the concentration of free carbodiimide is lower early in the experiment, in line with the results from the Ac system. Similarly, the longer lifetime is consistent with slowly released carbodiimide from the adduct over an extended period, giving an extended plateau of  $G'$ .

In summary, the formation of carbodiimide–pyridine adducts from mEDC is orthogonal to carbodiimide-driven anhydride formation. Pyridine additives therefore control the availability of carbodiimide, decreasing activation rates and prolonging anhydride lifetimes. In a transient hydrogel as a representative functional material, the time to peak modulus increased by 86% and the lifetime was extended by 43% for an mEDC/4-methoxypyridine system compared to the EDC control. This strategy should be generally useful as a way to control the kinetics of carbodiimide-driven chemical systems by expanding the reaction network.



## Funding Sources

This work was supported by United States Department of Energy, Office of Science, Basic Energy Sciences, under Award No. DE-SC0018645.

## Author Contributions

WSS was involved with methodology, validation, conceptualization, formal analysis, data curation, visualization, and writing the first draft. GM, NKS, CWHR were each involved with methodology, validation, formal analysis, data curation, and editing. DK was involved in conceptualization, formal analysis, and editing. CSH was involved in conceptualization, formal analysis, supervision, and editing.

## References

- (1) Boekhoven, J.; Hendriksen, W. E.; Koper, G. J. M.; Eelkema, R.; van Esch, J. H. Transient Assembly of Active Materials Fueled by a Chemical Reaction. *Science* **2015**, *349* (6252), 1075–1079. <https://doi.org/10.1126/science.aac6103>.
- (2) Wilson, M. R.; Solà, J.; Carlone, A.; Goldup, S. M.; Lebrasseur, N.; Leigh, D. A. An Autonomous Chemically Fuelled Small-Molecule Motor. *Nature* **2016**, *534* (7606), 235–240. <https://doi.org/10.1038/nature18013>.
- (3) Kariyawasam, L. S.; Hossain, M. M.; Hartley, C. S. The Transient Covalent Bond in Abiotic Nonequilibrium Systems. *Angew. Chem. Int. Ed.* **2021**, *60* (23), 12648–12658. <https://doi.org/10.1002/anie.202014678>.
- (4) Ogden, W. A.; Guan, Z. Redox Chemical-Fueled Dissipative Self-Assembly of Active Materials. *ChemSystemsChem* **2020**, *2* (4), e1900030. <https://doi.org/10.1002/syst.201900030>.
- (5) Del Giudice, D.; Di Stefano, S. Dissipative Systems Driven by the Decarboxylation of Activated Carboxylic Acids. *Acc. Chem. Res.* **2023**, *56* (7), 889–899. <https://doi.org/10.1021/acs.accounts.3c00047>.
- (6) Tena-Solsona, M.; Rieß, B.; Grötsch, R. K.; Löhner, F. C.; Wanzke, C.; Käsdorf, B.; Bausch, A. R.; Müller-Buschbaum, P.; Lieleg, O.; Boekhoven, J. Non-Equilibrium Dissipative Supramolecular Materials with a Tunable Lifetime. *Nat. Commun.* **2017**, *8* (1), 15895. <https://doi.org/10.1038/ncomms15895>.
- (7) Kariyawasam, L. S.; Hartley, C. S. Dissipative Assembly of Aqueous Carboxylic Acid Anhydrides Fueled by Carbodiimides. *J. Am. Chem. Soc.* **2017**, *139* (34), 11949–11955. <https://doi.org/10.1021/jacs.7b06099>.
- (8) Bai, S.; Niu, X.; Wang, H.; Wei, L.; Liu, L.; Liu, X.; Eelkema, R.; Guo, X.; van Esch, J. H.; Wang, Y. Chemical Reaction Powered Transient Polymer Hydrogels for Controlled Formation and Free Release of Pharmaceutical Crystals. *Chem. Eng. J.* **2021**, *414*, 128877. <https://doi.org/10.1016/j.cej.2021.128877>.
- (9) Zhang, B.; Jayalath, I. M.; Ke, J.; Sparks, J. L.; Hartley, C. S.; Konkolewicz, D. Chemically Fueled Covalent Crosslinking of Polymer Materials. *Chem. Commun.* **2019**, *55* (14), 2086–2089. <https://doi.org/10.1039/C8CC09823A>.
- (10) Rajawasam, C. W. H.; Tran, C.; Weeks, M.; McCoy, K. S.; Ross-Shannon, R.; Dodo, O. J.; Sparks, J. L.; Hartley, C. S.; Konkolewicz, D. Chemically Fueled Reinforcement of Polymer Hydrogels. *J. Am. Chem. Soc.* **2023**, *145* (9), 5553–5560. <https://doi.org/10.1021/jacs.3c00668>.

- (11) Bal, S.; Das, K.; Ahmed, S.; Das, D. Chemically Fueled Dissipative Self-Assembly That Exploits Cooperative Catalysis. *Angew. Chem. Int. Ed.* **2019**, *58* (1), 244–247. <https://doi.org/10.1002/anie.201811749>.
- (12) Bal, S.; Ghosh, C.; Ghosh, T.; Vijayaraghavan, R. K.; Das, D. Non-Equilibrium Polymerization of Cross- $\beta$  Amyloid Peptides for Temporal Control of Electronic Properties. *Angew. Chem. Int. Ed.* **2020**, *59* (32), 13506–13510. <https://doi.org/10.1002/anie.202003721>.
- (13) Donau, C.; Boekhoven, J. The Chemistry of Chemically Fueled Droplets. *Trends Chem.* **2023**, *5* (1), 45–60. <https://doi.org/10.1016/j.trechm.2022.11.003>.
- (14) Binks, L.; Borsley, S.; Gingrich, T. R.; Leigh, D. A.; Penocchio, E.; Roberts, B. M. W. The Role of Kinetic Asymmetry and Power Strokes in an Information Ratchet. *Chem* **2023**, *9* (10), 2902–2917. <https://doi.org/10.1016/j.chempr.2023.05.035>.
- (15) Borsley, S.; Leigh, D. A.; Roberts, B. M. W. A Doubly Kinetically-Gated Information Ratchet Autonomously Driven by Carbodiimide Hydration. *J. Am. Chem. Soc.* **2021**, *143* (11), 4414–4420. <https://doi.org/10.1021/jacs.1c01172>.
- (16) Borsley, S.; Kreidt, E.; Leigh, D. A.; Roberts, B. M. W. Autonomous Fuelled Directional Rotation about a Covalent Single Bond. *Nature* **2022**, *604* (7904), 80–85. <https://doi.org/10.1038/s41586-022-04450-5>.
- (17) Borsley, S.; Leigh, D. A.; Roberts, B. M. W.; Vitorica-Yrezabal, I. J. Tuning the Force, Speed, and Efficiency of an Autonomous Chemically Fueled Information Ratchet. *J. Am. Chem. Soc.* **2022**, *144* (37), 17241–17248. <https://doi.org/10.1021/jacs.2c07633>.
- (18) Jayalath, I. M.; Wang, H.; Mantel, G.; Kariyawasam, L. S.; Hartley, C. S. Chemically Fueled Transient Geometry Changes in Diphenic Acids. *Org. Lett.* **2020**, *22* (19), 7567–7571. <https://doi.org/10.1021/acs.orglett.0c02757>.
- (19) Jayalath, I. M.; Gerken, M. M.; Mantel, G.; Hartley, C. S. Substituent Effects on Transient, Carbodiimide-Induced Geometry Changes in Diphenic Acids. *J. Org. Chem.* **2021**, *86* (17), 12024–12033. <https://doi.org/10.1021/acs.joc.1c01385>.
- (20) Hossain, M. M.; Jayalath, I. M.; Baral, R.; Hartley, C. S. Carbodiimide-Induced Formation of Transient Polyether Cages. *ChemSystemsChem* **2022**, *4* (6), e202200016. <https://doi.org/10.1002/syst.202200016>.
- (21) Dodo, O. J.; Petit, L.; Rajawasam, C. W. H.; Hartley, C. S.; Konkolewicz, D. Tailoring Lifetimes and Properties of Carbodiimide-Fueled Covalently Cross-Linked Polymer Networks. *Macromolecules* **2021**, *54* (21), 9860–9867. <https://doi.org/10.1021/acs.macromol.1c01586>.
- (22) Heckel, J.; Batti, F.; Mathers, R. T.; Walther, A. Spinodal Decomposition of Chemically Fueled Polymer Solutions. *Soft Matter* **2021**, *17* (21), 5401–5409. <https://doi.org/10.1039/D1SM00515D>.
- (23) Stasi, M.; Monferrer, A.; Babl, L.; Wunnava, S.; Dirscherl, C. F.; Braun, D.; Schwill, P.; Dietz, H.; Boekhoven, J. Regulating DNA-Hybridization Using a Chemically Fueled Reaction Cycle. *J. Am. Chem. Soc.* **2022**, *144* (48), 21939–21947. <https://doi.org/10.1021/jacs.2c08463>.
- (24) Mondal, S.; Halder, D. A Transient Non-Covalent Hydrogel by a Supramolecular Gelator with Dynamic Covalent Bonds. *New J. Chem.* **2021**, *45* (10), 4773–4779. <https://doi.org/10.1039/D0NJ05992G>.
- (25) Cheng, M.; Qian, C.; Ding, Y.; Chen, Y.; Xiao, T.; Lu, X.; Jiang, J.; Wang, L. Writable and Self-Erasable Hydrogel Based on Dissipative Assembly Process from Multiple Carboxyl



- Tetraphenylethylene Derivative. *ACS Mater. Lett.* **2020**, *2* (4), 425–429. <https://doi.org/10.1021/acsmaterialslett.9b00509>.
- (26) Ibrahim, I. T.; Williams, A. Reaction of the Water-Soluble Reagent N-Ethyl-N'-(3-Dimethylaminopropyl)Carbodiimide with Nucleophiles: Participation of the Tautomeric Cyclic Ammonioamidine as a Kinetically Important Intermediate. *J. Am. Chem. Soc.* **1978**, *100* (23), 7420–7421. <https://doi.org/10.1021/ja00491a053>.
- (27) Tenforde, T.; Fawwaz, R. A.; Freeman, N. K.; Castagnoli, N. Jr. Nuclear Magnetic Resonance and Infrared Studies on the Tautomerism of 1-Ethyl-3-(3'-Dimethylaminopropyl)Carbodiimide. *J. Org. Chem.* **1972**, *37* (21), 3372–3374. <https://doi.org/10.1021/jo00986a049>.
- (28) Williams, A.; Ibrahim, I. T. A New Mechanism Involving Cyclic Tautomers for the Reaction with Nucleophiles of the Water-Soluble Peptide Coupling Reagent 1-Ethyl-3-(3'-(Dimethylamino)Propyl)Carbodiimide (EDC). *J. Am. Chem. Soc.* **1981**, *103* (24), 7090–7095. <https://doi.org/10.1021/ja00414a011>.
- (29) Kariyawasam, L. S.; Kron, J. C.; Jiang, R.; Sommer, A. J.; Hartley, C. S. Structure–Property Effects in the Generation of Transient Aqueous Benzoic Acid Anhydrides by Carbodiimide Fuels. *J. Org. Chem.* **2020**, *85* (2), 682–690. <https://doi.org/10.1021/acs.joc.9b02746>.
- (30) Kriebisch, B. A. K.; Jussupow, A.; Bergmann, A. M.; Kohler, F.; Dietz, H.; Kaila, V. R. I.; Boekhoven, J. Reciprocal Coupling in Chemically Fueled Assembly: A Reaction Cycle Regulates Self-Assembly and Vice Versa. *J. Am. Chem. Soc.* **2020**, *142* (49), 20837–20844. <https://doi.org/10.1021/jacs.0c10486>.
- (31) Bonora, M.; Patergnani, S.; Rimessi, A.; De Marchi, E.; Suski, J. M.; Bononi, A.; Giorgi, C.; Marchi, S.; Missiroli, S.; Poletti, F.; Wieckowski, M. R.; Pinton, P. ATP Synthesis and Storage. *Purinergic Signal.* **2012**, *8* (3), 343–357. <https://doi.org/10.1007/s11302-012-9305-8>.
- (32) Wang, Z.; Cole, P. A. Catalytic Mechanisms and Regulation of Protein Kinases. *Methods Enzymol.* **2014**, *548*, 1–21. <https://doi.org/10.1016/B978-0-12-397918-6.00001-X>.
- (33) Schirmer, A.; Kennedy, J.; Murli, S.; Reid, R.; Santi, D. V. Targeted Covalent Inactivation of Protein Kinases by Resorcylic Acid Lactone Polyketides. *Proc. Natl. Acad. Sci. U. S. A.* **2006**, *103* (11), 4234–4239. <https://doi.org/10.1073/pnas.0600445103>.
- (34) Chen, X.; Soria-Carrera, H.; Zozulia, O.; Boekhoven, J. Suppressing Catalyst Poisoning in the Carbodiimide-Fueled Reaction Cycle. *Chem. Sci.* **2023**, *14* (44), 12653–12660. <https://doi.org/10.1039/D3SC04281B>.
- (35) Vovk, M. V.; Lebed', P. S.; Chernega, A. N.; Pirozhenko, V. V. Unusual Cyclization of N-(1-Aryl-1-Chloro-2, 2, 2-Trifluoroethyl)-N'-(p-Tolyl)-Carbodiimides in the Presence of Triethylamine. *Russ. J. Org. Chem.* **2002**, *40* (2), 195–198.
- (36) Bhattacharjee, J.; Harinath, A.; Banerjee, I.; Nayek, H. P.; Panda, T. K. Highly Active Dinuclear Titanium(IV) Complexes for the Catalytic Formation of a Carbon–Heteroatom Bond. *Inorg. Chem.* **2018**, *57* (20), 12610–12623. <https://doi.org/10.1021/acs.inorgchem.8b01766>.
- (37) Zhu, T.-H.; Wang, S.-Y.; Tao, Y.-Q.; Ji, S.-J. Synthesis of Carbodiimides by I<sub>2</sub>/CHP-Mediated Cross-Coupling Reaction of Isocyanides with Amines under Metal-Free Conditions. *Org. Lett.* **2015**, *17* (8), 1974–1977. <https://doi.org/10.1021/acs.orglett.5b00722>.

- (38) DMAP was also tested but fails to give adduct, presumably because it is predominantly protonated at the pH's investigated.
- (39) Hansch, Corwin.; Leo, A.; Taft, R. W. A Survey of Hammett Substituent Constants and Resonance and Field Parameters. *Chem. Rev.* **1991**, *91* (2), 165–195. <https://doi.org/10.1021/cr00002a004>.
- (40) Fersht, A. R.; Jencks, W. P. Acetylpyridinium Ion Intermediate in Pyridine-Catalyzed Hydrolysis and Acyl Transfer Reactions of Acetic Anhydride. Observation, Kinetics, Structure-Reactivity Correlations, and Effects of Concentrated Salt Solutions. *J. Am. Chem. Soc.* **1970**, *92* (18), 5432–5442. <https://doi.org/10.1021/ja00721a023>.
- (41) Bunton, C. A.; Perry, S. G. The Acid-Catalysed Hydrolysis of Carboxylic Anhydrides. *J. Chem. Soc. Resumed* **1960**, No. 0, 3070–3079. <https://doi.org/10.1039/JR9600003070>.